

# Policy Gradient Approach to Compilation of Variational Quantum Circuits

D. A. Herrera-Martí<sup>1</sup>

<sup>1</sup> *Université Grenoble Alpes, CEA List, 38000 Grenoble, France*

(Dated: April 29, 2022)

We propose a method for finding approximate compilations of quantum unitary transformations, based on techniques from policy gradient reinforcement learning. The choice of a stochastic policy allows us to rephrase the optimization problem in terms of probability distributions, rather than variational gates. In this framework, finding the optimal configuration is done by optimizing over distribution parameters, rather than over free angles. We show numerically that this approach can be more competitive than gradient-free methods, for comparable amounts of resources (*i.e.* quantum circuit runs). Another interesting feature of this approach to variational compilation is that it does not need a separate register and long-range interactions to estimate the end-point fidelity, which is an improvement over methods which rely on the Hilbert-Schmidt test. We expect these techniques to be relevant for training variational circuits in other contexts.

## I. INTRODUCTION

The general problem of quantum compilation is to approximate any unitary transformation with a sequence of elements selected from a fixed universal set of quantum gates. The existence of an approximate sequence of quantum gates for a single qubit is guaranteed by the Solovay-Kitaev theorem [1], which states that any single-qubit gate can be approximated with an overhead logarithmic in the original number of gates, *i.e.* polylogarithmic as  $O(\log^c(1/\epsilon))$ , where  $\epsilon$  is the approximation accuracy and  $c$  is a constant lower-bounded by 1 [2].

Although the Solovay-Kitaev theorem proves that any computation can be efficiently approximated to within an arbitrary tolerance, it does not tell us how to find the optimal sequence of gates. The standard algorithm uses an exhaustive search technique to build a library of gate sequences in its lowest level of recursion, and then builds on it recursively. In general, the longer the sequence of library gates (and their inverses), the better the approximation to the target unitary [3].

Finding the optimal compilation of a quantum unitary is equivalent to finding the shortest path between two nodes (the geodesic) in a (hyperbolic) Cayley graph [4]. Hyperbolic graphs resemble tree graphs in the sense that for an overwhelming majority of node pairs, there is only one path linking both nodes [5]. Therefore, the geometric intuition for the hardness of exact compilation is that, in a hyperbolic graph, looking for a shortest path involves evaluating an exponential number of nodes at each step. Indeed, performing an optimal compilation of a given quantum circuit is believed to be a hard problem under reasonable assumptions [4, 6].

With the advent of sub-threshold quantum architectures [7], research on variational quantum algorithms has become central to the field of quantum computing, giving rise, among others, to alternative routes to universal quantum computation, based on variational circuits [8–10]. The existence of variational tasks which are believed to be intractable for classical computers [11–16] is an encouraging motivation for research in variational

quantum algorithms. By considering a discretization of the rotation angles, which are the free variational parameters, it can be seen that the set of circuits that can be built using these gates has a Cayley graph which retains its hyperbolic character [4], and therefore this method of compilation is likely to be suboptimal for large unitaries.

Furthermore, several bottlenecks must be addressed before variational quantum algorithms on a NISQ processor can be properly trained at scale. These include the ability to evaluate efficiently cost functions which are made of non-commuting observables [17, 18], and the design of new algorithms with no known efficient classical simulation [19–21], in which the optimizations of the variational parameters may suffer from the curse of dimensionality as the number of qubits increases.

A further impediment to VQA training is due to the fact that there are regions in parameter space, commonly known as *barren plateaus*, where the cost gradient vanishes exponentially in the number of qubits. This behaviour of the cost function, which exponentially increases the resources required to train large scale quantum neural networks, is a manifestation of the concentration of measure phenomenon and it has been demonstrated in a number of proposed architectures and classes of cost functions [22, 23]. Similarly, gradient-free optimizers are unable to weather the barren plateau problem, as finite differences on which their iterative improvements are based, are exponentially suppressed in a barren plateau [30].

Several strategies have been suggested to mitigate the effect of barren plateaus during the training of variational quantum circuits. Some techniques aim at circumventing the probabilistic independence assumption which underlies the concentration results [24, 25], while others try to train the circuit piecewise or using subensembles of angles [23, 26]. Although each of these methods has advantages and drawbacks, no fully satisfactory solution to this problem has yet been devised. In this work, we explore ideas from reinforcement learning, and in particular policy gradient methods, to mitigate the effects of barren plateaus in the training of variational quantum algorithms of shallow depth (logarithmic in the num-

ber of qubits), and we apply it to the particular case of approximate compilation. The intuition behind this choice comes given by the fact that in policy gradient algorithms, the cost function can be written as an expected value of a parameterized analytic function. This means that an update rule can be defined which involves sampling potential configurations in the local neighborhood of the current solution. The size of this neighborhood can be tuned dynamically by changing the update stride (see Appendix A). We show that this approach is competitive and that it can outperform gradient-based methods in noiseless and noisy circuits at the onset of a barren plateau.

## II. COMPILATION OF VARIATIONAL QUANTUM ALGORITHMS

The goal is to learn the action of an unknown unitary gate  $U$  on an arbitrarily large set of initial states (see Fig. 1). The first assumption we make is that  $U$  is at most of logarithmic depth, which is motivated by the fact that in NISQ architectures (in the absence of error correction) this is already a beneficial scaling, and by the fact that barren plateaus will arise for global cost functions, as in that in Eq.1 ([23]). Our second working hypothesis is that the interactions giving rise to the unknown unitary, i.e. the qubit connectivity graph, are known. We have assumed that they are nearest-neighbors, but more general interactions are straightforward, provided that the interaction graph is known to the compiler. In the absence of all information, an all-to-all circuit should be trained, which would entail a quadratic growth of number of free parameters in the number of qubits, and having to optimize over extra spurious angles would reduce the interest of this method.

There are several approaches [8, 10, 27, 28] to assess the performance of an approximate compilation method. We will adopt a variation of one metric introduced in Refs. [27, 28], motivated by its experimental feasibility:

$$\hat{F}(\theta) = \frac{1}{m} \sum_k^m |\langle k|V(\theta)^\dagger U|k\rangle|^2 \quad (1)$$

which corresponds to the fidelity between the initial and the final state. To fully characterize  $U$ , a tomographically complete characterization demands  $\mathcal{O}(4^n)$  different such initial states. Variational quantum compiling of a full unitary matrix  $U$  by considering the action of  $U$  on a complete basis gets computationally very demanding very rapidly as the number of qubits grows. A simpler task is to learn to prepare only a particular column of the matrix  $U$  by considering the action of  $U$  on a fixed input state, or on a small subset of initial states. The Hilbert-Schmidt test in [27, 28] has the advantage that it estimates the gate similarity  $\text{Tr}[V(\theta)^\dagger U]$ , at the cost of doubling the number of qubits and introducing highly

non-local interactions. In this work, we will estimate the fidelity using only  $m \sim \text{poly}(n)$  initial states and  $n$  qubits (see Appendix B), a fact which is denoted by the hat punctuation in previous equation.

Approximate compilation of random unitaries, phrased as a variational algorithm, will necessarily get stuck in barren plateaus [32]. We will try to mitigate this problem using a optimizing a stochastic version of the cost function stated on Eq. (1).

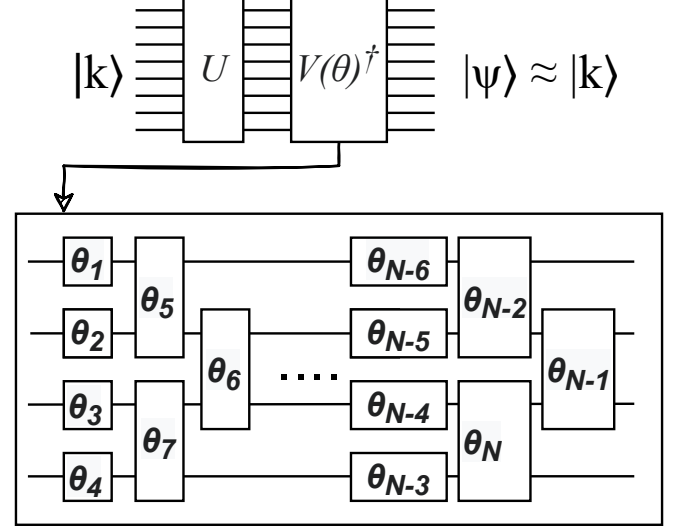


FIG. 1. Circuit Setup. The goal is to retrieve a state with a maximal overlap with the initial state  $|k\rangle$ , for all initial states, randomly sampled from a fixed basis. The unknown unitary  $U$  is followed by  $V(\theta)^\dagger$ , resulting in a state  $|\psi\rangle$ . At the end of the circuit, the measurement projects the state back onto the initial state with a probability that depends on the overlap, which constitutes the reward, i.e.  $r_\theta^{(k)} = |\langle k|V(\theta)^\dagger U|k\rangle|^2$ . The parameterized unitary is made of single qubit rotations of the form  $R_Y(\theta_i) = \exp -iY\theta_i$  and two-qubit rotations are of the form  $R_{ZZ}(\theta_i) = \exp -iZZ\theta_i$ .

## III. POLICY GRADIENT FOR QUANTUM COMPILATION

Policy Gradient (PG) Reinforcement Learning (RL) operates on the premise that it is possible to optimize a parametric policy by probing the environment, without the need of continuous update of policy surrogate functions, and it constitutes an alternative to Q-learning algorithms [33]. PGRL is naturally well suited to handle continuous actions in stochastic environments and, provided that the chosen policy is differentiable, the gradient of a cost function can always be estimated. The bias incurred by this method will also be related to the expressive power of the chosen policy (see Fig. 2). RL has found multiple applications for several quantum tasks such as code design [34], single qubit unitary compilation [35], feedback control [36, 37] or state preparation [38].

Of particular interest are several works where the possibility of automatically learning how to optimize variational quantum algorithms [39–42] has been addressed. Interestingly, PG algorithms for variational quantum algorithms have been shown to be robust against noise, and they can systematically outperform other methods in the training of small noisy circuits for combinatorial optimization. In this work we explore a regime of shallow circuits with an increasing number of qubits, a regime complementary to that explored in [40], where they focus on a QAOA ansatz for a small number of qubits.

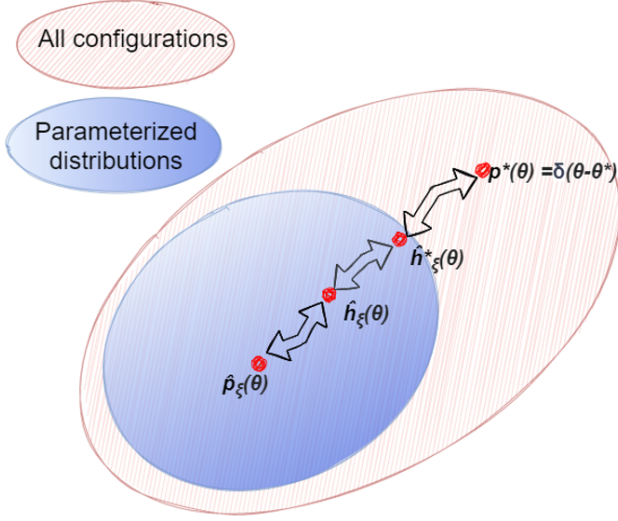


FIG. 2. Expressivity of the model as a function of the chosen policy. A given set of probability distributions parameterized by a vector  $\xi$  is contained in the larger set of all probability distributions. The statistical distance which separates the learned distribution from the ground truth has three components. The **training error**, which underlies the optimization method, is the statistical distance between the current distribution  $\hat{p}_\xi(\theta)$  and the empirically optimal hypothesis  $\hat{h}_\xi(\theta)$ . The distance between the empirically optimal hypothesis and the optimal hypothesis  $h_\xi^*(\theta)$  comes given by the **finiteness of sampling**. Finally, the distance between  $h^*(\theta)$  and the ground truth  $p^*(\theta) = \delta(\theta - \theta^*)$  depends on the **model expressivity** of the chosen parameterization. Updates within the parameterized set correspond to finding a stochastic policy with the smallest distance to the ground truth.

In order to properly use RL in solving a quantum task, the agent’s state, its available set of actions and the sampled reward need to be precisely defined (see Appendix A). In our case, the RL state will correspond to the quantum wavefunction, the set of possible actions  $\theta = (\theta_1, \theta_2, \dots, \theta_N)$  will be the set of free angles in  $V(\theta)$ , and the reward will be proportional to the state fidelity. The simplest PGRL algorithm, known as REINFORCE [45], draws extensively from Monte-Carlo learning, where episodes correspond to sampling at once all possible actions and then the performance is measured as the episode unravels [33].

### A. REINFORCE with Endpoint Rewards

As motivated above, the REINFORCE algorithm can be slightly modified so that the reward is only related to the measured fidelity at the end of each circuit, meaning that for we need not worry about performing intermediate measurements which would collapse the wavefunction and interrupt the computation. The reward will be the overlap between the initial and the final state, given by Eq.(1). During this first exploration of this approach, the set of possible actions  $\theta = (\theta_1, \theta_2, \dots, \theta_N)$  under the current policy, i.e. the angles of 1- and 2-qubit gates ( $R_Y$  and  $R_{ZZ}$  gates), will be randomly sampled from a Gaussian distribution of the form (see Fig. 1):

$$\theta \sim \pi(x; \mu, \Sigma) = \frac{1}{\sqrt{2\pi|\Sigma|}} e^{-(x-\mu)\Sigma^{-1}(x-\mu)^T} \quad (2)$$

where the covariance matrix  $\Sigma$  can either be fixed or obey some exploration-exploitation schedule, or it might even be learnt (see Appendix A). The corresponding objective function is:

$$J = \mathbb{E}_{\pi_\mu}[F] = \sum_k p_k \sum_\theta \pi(\theta|\mu, \Sigma) |\langle k|V(\theta)^\dagger U|k \rangle|^2 \quad (3)$$

which corresponds to an average of the endpoint reward, i.e the asymptotic fidelity, over initial states (each sampled with probability  $p_k$ ) and all possible actions (given by the current policy  $\pi(\theta|\mu, \Sigma)$ ). In our case, maximizing  $J$  corresponds to minimizing the associated cost function  $J = \mathbb{E}_{\pi_\mu}[F] \xrightarrow{|\Sigma| \rightarrow 0} 1 - C$ .

The gradient of function in Eq.(3) is therefore:

$$\nabla_\mu J = \sum_k p_k \sum_\theta \pi(\theta|\mu, \Sigma) \nabla_\mu \log \pi(\theta|\mu, \Sigma) |\langle k|V(\theta)^\dagger U|k \rangle|^2 \quad (4)$$

where we have used the so-called “policy gradient trick”, which amounts to applying the chain rule to the policy function, and allows to write the gradient of an expectation value as the expectation of a loglikelihood times a cost function [33]. Estimating the gradient thus reduces to sampling a few episodes, i.e. performing several Monte-Carlo tree searches, and evaluating the cost function at the end of each one (see Appendix A).

### B. Random Walking over the Edge

The cost landscape in many variational task is expected to become exponentially flat (in the number of qubits) except around some narrow gorges leading to good configurations. If during an optimization the candidate solution finds itself in a non-zero slope region, sampling action configurations will very rapidly lead to non-vanishing gradients. One useful way of thinking about

the Gaussian policy  $\pi(\theta; \mu, \Sigma)$  is as quantifying the probability of obtaining a configuration that at some distance from a minimum at location  $\mu$ . With this parameterization, the RL problem will learn to place  $\mu$  as close as possible to the nearest minimum in the current non-zero slope region.

If, on the contrary, the current  $\mu$  is in a flat region, which is overwhelmingly more likely to happen, it will be very far away in Euclidean distance from any minimum. Here we do not expect this method to perform better than average as the dimensionality grows. In this case the gradient will consist of a (constant) cost times an empirical expectation of a Gaussian displacement:

$$\begin{aligned} \nabla_{\mu} J &= \sum_{\theta} \sum_k^m p_k \pi(\theta|\mu, \Sigma) \nabla_{\mu} \log \pi(\theta|\mu, \Sigma) |\langle k|V(\theta)^{\dagger}U|k \rangle|^2 \\ &\approx \frac{1}{N_{eps}} \sum_{\theta} [\Sigma^{-1}(\theta - \mu)] \times \epsilon \end{aligned} \quad (5)$$

where the constant  $\epsilon$  corresponds to the fidelity evaluated in the flat region. This will lead to a random walk for which one can compute the mean square displacement to be  $\sim \eta \epsilon \sqrt{\frac{N_{iters}}{N_{eps}}} \text{Tr} \Sigma^{-1}$ , with  $\eta$  the learning rate of the gradient descent algorithm (see Appendices A and C) and  $1/N_{iters}$  the discretized time lapse. As explained in the Appendices, the counterintuitive presence of an inverse covariance in the mean square displacement is due to the fact that the update rule is inversely proportional to the policy's current covariance, as it would otherwise favour configurations that are frequently sampled, rather than those with high rewards [33]. We have numerically verified that, for initializations within flat cost landscapes, performance of PG gets degraded as the eigenvalues of covariance matrix  $\Sigma$  grow, in accordance to the expression for the mean-squared displacement in Appendix C. This random walk evolves within a hyperball with radius increasing roughly as  $\sim \sqrt{N_q D N_{iters}}$ . However, since the volume ratio between of a hyperball of radius and its corresponding hypercube vanishes with a factorial dependence on the dimensionality, this approach is expected to stall deep inside a barren plateau.

The regions of interest are in the cross-over between the two regimes. In those regions (i.e. at the edge of, yet within a flat landscape) PG-based training can “feel” a change in slope if allowed to diffuse for sufficiently long. In Fig.3 we illustrate this region where enhanced performance is expected, where the candidate solution random-walks over the edge and enters a non-zero slope region.

We argue that the correct ensemble of benchmarks for this method are gradient-free optimisers, as opposed to gradient-based methods (based for instance on the parameter-shift rule [31]). Contrary to what happens in classical neural networks (where backpropagation can be used), the gradient calculated in VQAs needs to be done using several of the equivalent of forward-backward passes, which amounts to computing commutators with

some real or fiducial Hamiltonian (see for example [28]). This means that, for each iteration, one commutator per free parameter has to be evaluated. Moreover, this evaluation needs to be done within a fixed tolerance, so the number of measurements per commutator grows with as the inverse tolerance squared times the number of free parameters. On top of this, PG optimization of variational algorithms is a non-local optimization procedure, since estimating the gradient of the cost function involves sampling episodes in the vicinity of the current tentative solution. This is aligned in philosophy with gradient-free optimizers which sample finite differences relative to different locations in parameter space, rather than gradient descent, in which gradient is evaluated at a single point in parameter space at each iteration.

Our aim will therefore be to empirically compare the performance of PG-based variational compilation with that of gradient-free methods.

#### IV. NUMERICAL EXPERIMENTS AND RESULTS

To assess the performance of PG methods applied to variational compilation, we have run numerical simulations of the training procedure, both in the noiseless case and for noisy circuits. We generated several random shallow quantum circuits with depth logarithmic in the number of qubits and known connectivity graph, which acted as the target unitary  $U$ , followed by a circuit with the same connectivity graph and depth, and randomized parameters implementing another unitary  $V$ . As hinted previously, this setup is physically motivated because in the absence of error correction, circuit depth of NISQ algorithms is bounded by the inverse effective noise rate, which means that only shallow circuits, i.e. of constant depth, can be realistically considered [14, 15]. Moreover, the logarithmic depth regime is expected to suffer from the barren plateau effect for global cost functions [23].

Practically, our choice for this setup stems from the need to evaluate how close the performance gets to its theoretical maximum. Given that most unitaries have exponentially long circuits [1], sampling operators in  $SU(2^n)$ , instead of explicitly defining a quantum circuit, would almost surely result in the optimization getting stuck at indeterminate values of the cost function, which would in turn lead to a poor characterization of the performance.

Our methodology consisted of testing different gradient-free methods, such as Powell (which relies on bi-directional search) and COBYLA (simplex-based), and a simple variations of REINFORCE PG, and to compare their relative performance in training  $V(\theta)$  to act as much as possible as the inverse of the target unitary, i.e to determine  $\theta^*$  such that  $V(\theta^*) = U^{\dagger}$ . We used the *Cirq* simulator for this purpose [46].

In order to establish a meaningful comparison between PG-based training and gradient-free optimisers, it is nec-

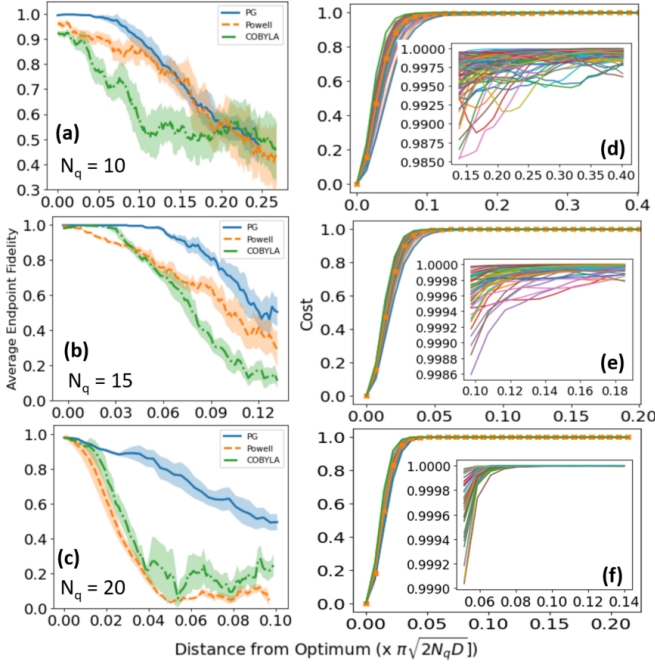


FIG. 3. Performance, measured as the asymptotic reward, as a function of the initialization distance  $d = |\hat{\theta} - \theta^*|/(\pi\sqrt{2N_qD})$  over the torus. Several circuits were run for increasing distances and moving averages taken over the whole sequence of (a) 200 runs for  $N_q = 10$  and  $D = 3$ , (b) 100 runs for  $N_q = 15$  and  $D = 4$ , and (c) 50 runs for  $N_q = 20$  and  $D = 5$ . The shadows correspond to one moving standard deviation. PG with endpoint rewards typically performs better than COBYLA and Powell optimisers. Our numerics show that the improvement in performance becomes more dramatic as the number of qubits grows, which can be seen as evidence that whereas gradient-free methods are unable to move in the correct direction near the onset of the barren plateau, PG updates in the diffusive regime allows to explore increasingly far configurations and eventually find a non-zero slope region (see Fig.4). (d-f) Numerically computed cross-sections along random directions of the cost landscape. The gorge corresponding to the global optimum gets narrower as the number of qubit increases. Insets: the exponential reduction of the cost variance. Whereas for (d) 10 qubits the fluctuations in the cost remain in the order of 1%, which can be fully exploited by gradient-free optimisers, for (f) 20 qubits the cost fluctuations rapidly descend well below  $10^{-4}$ .

essary to quantify the resources that either method needs to converge. Each iteration of a gradient-free optimiser entails a fixed number of runs ( $n_{shots}$ ) of a quantum processor. In PG-based training, each episode involves sampling a few configurations in the vicinity of the current configuration to estimate the gradient, so the number of runs is  $n_{shots} \times N_{eps}$ . There are two factors that render the comparison difficult. The first one is that the learning rate is a hyperparameter that can be tuned, and the number of iterations depends heavily on it. The second consideration is that PG-based training is robust to fluctuations (see Appendix D), so its performance is not

degraded as much as that of gradient-free optimisers as  $n_{shots}$  is reduced (see Fig. 5). As a general rule, we have set a maximum number of iterations to a sufficiently large value so that COBYLA and Powell typically converge (either to good or bad solutions). We found empirically this to grow very fast on the number of qubits, from about a few hundred iterations for 10 qubits to about  $\sim 10^4$  for 20 qubits.

#### A. Performance vs Distance from Optimum

The trainability of variational circuits, measured in terms of the obtained reward, as a function of the distance  $r$  from the optimum is shown in Fig.3. The performance of policy gradient is degraded further away from the optimum, albeit significantly less than for gradient-free optimizers, as the tentative solution is initialized further and further from the optimum. We interpret this as a consequence of the PG algorithm entering a “diffusive regime” in which the tentative solution performs a random walk and at some point falls over the edge. Evidence for this behaviour is provided by the trajectories shown in Fig.4. There, one can see that whereas simplex-based methods are unable to move in the correct directions if initialized too far from the optimum. (cf. [30]).

Gradient-based optimizers will also perform a random walk in a barren plateau if the magnitude of the gradient is too small compared to the measurement precision [26], however this behaviour only depends on evaluations of the gradient at a single point in parameter space. On the contrary, the random walk performed by the REINFORCE algorithm will explore configurations in a non-local way (by sampling episodes at in the vicinity the current configuration), whose performances are then averaged and used to perform an update.

#### B. Training Noisy Circuits

Noise can be shown to impose an upper bound on the gradient strength and it further hinders trainability of variational quantum circuits of linear depth[29]. We have sought to estimate the robustness of the method in the presence of noise in the logarithmic depth regime. Noise simulations involved appending a single-qubit depolarizing channel after each single qubit gate. After each depolarizing channel, the average loss of fidelity comes given by  $(1 - p)$ , so after  $D$  layers, the fidelity will decrease on average by  $(1 - p)^{N_q D}$ , irrespective of the angle. Each of the episodes needed to estimate the gradient will sample a reward which will be reduced by the same factor on average. Being a stochastic update policy, PG is naturally robust against this kind of errors, so the search will proceed in correct direction, albeit with more variance and slower convergence (see Appendix D). Fig.5 depicts the relative performances of PG-based optimization, COBYLA and Powell in the presence of noise.



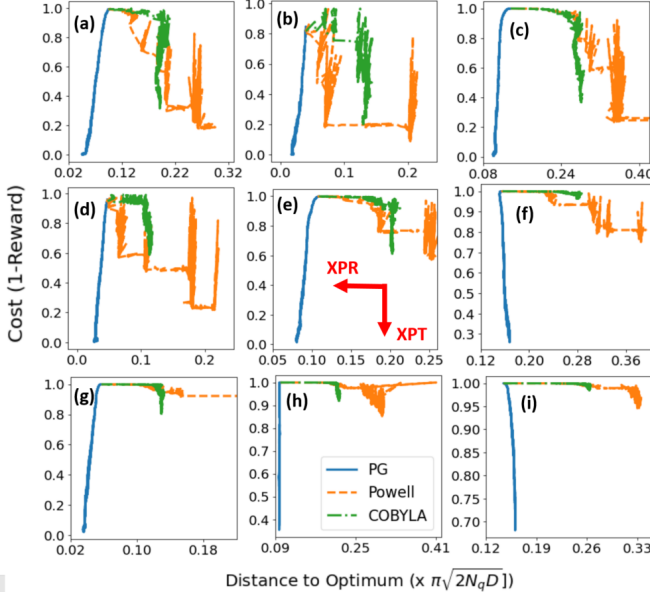


FIG. 4. Optimization trajectories, depicted in  $(\text{distance}, \text{cost})$ -coordinates for 10 (a-c), 15 (d-f) and 20 qubits (g-i) and approximate initialization distances 0.05 (a,d,g), 0.1 (b,e,h) and 0.15 (c,f,i). In these coordinates, it is possible to diagnose whether the optimization is in an exploration (XPR) or in an exploitation (XPT) phase. The exploration phase is characterized by searching for new configurations even if it does not result in a net cost reduction. Conversely, in an exploitation phase priority is given to updates which minimise the cost (see (e)). For a fixed number of 5000 runs per iteration, COBYLA and Powell optimisers are not able to “feel” the slope and rapidly get stuck in local minima. In subplots (f, h, i) the PG optimizer has clearly been trapped in a local minimum, as can be gleaned from the slope of the optimization trajectory. Whereas COBYLA, based on the simplex method, features a zig-zag behaviour typical of pivot operations, each iteration of the Powell method involves a line-wise minimization. Both of these optimizations are discrete in the sense that each update can bring the current configuration to a very different position in  $\theta$ -space. During PG-based learning, the candidate configuration is updated “continuously” if the learning rate is sufficiently small. This, together with the fact that, by tuning the covariance configurations beyond local maxima can be sampled, allows for a smoother optimization trajectory, resulting in a more balanced alternation between exploration and exploitation.

The observed behaviour in the numerics is again consistent with PG-based optimization as being able to find good solutions “at the edge” of a barren plateau even in the presence of noise. This can be understood as a consequence of the optimisation taking steps in the correct direction on average. If the step size  $\eta$  is sufficiently small, fluctuations will average out over successive steps.

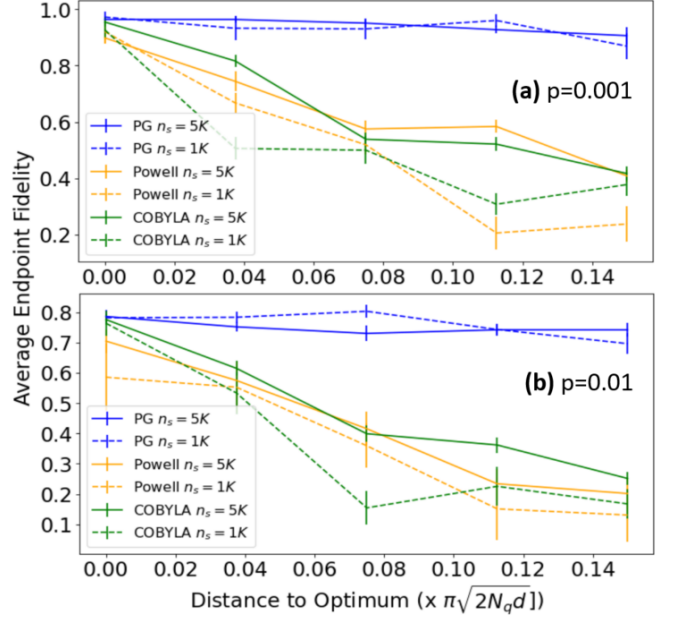


FIG. 5. Training of circuits of 10 qubits in the presence of depolarizing noise with probabilities (a)  $p = 0.01$  and (a)  $p = 0.001$  after each single qubit rotation. Each optimization was done for  $n_{shots} = 5000$  and  $n_{shots} = 1000$  per iteration. Error bars denote averaging over 10 optimizations. Compared to performances in see Fig. 3, one can see that PG is more robust than COBYLA and Powell methods in landscapes of non-zero slope. PG averages noise in gradients over successive updates, provided that noise is independent on  $\theta$  (see Appendix D). The damping of the endpoint fidelities is proportional to  $(1 - p)^{N_q D}$ . Increasing the number of runs can reduce the fluctuations at each step, leading to better convergence to the noisy maximum.

### C. Generalization Error

In order to estimate the gate the reward (circuit endpoint fidelity) without an acilliary register and long range interactions, which are needed to implement the Hilbert-Schmidt test [28, 29], we trained the circuit on small subsets of initial states to estimate the fidelity (see Appendix B). It is important to assess the generalization error of this method on states not included in the training of the variational circuit.

We trained several 10 qubit circuits on increasingly large sets of initial states, whose performance was then checked on different test sets as a function of the distance from the optimum. The training set was made of local quantum states of the form  $|k\rangle = \bigotimes_j^{10} R_Y(\frac{\pi}{4} \times c_j)|0\rangle_j$ , where  $c_j$  are random integers in the range  $[0, 2^3 - 1]$ . The circuit was tested on the  $|0\rangle$  state, which needed not be included in the training set, and two additional sets: one made of tensor product of local rotations and another one made of random state vectors (which are non-local with high probability). As shown in Fig. 6, the performance on test sets increases as the number of states

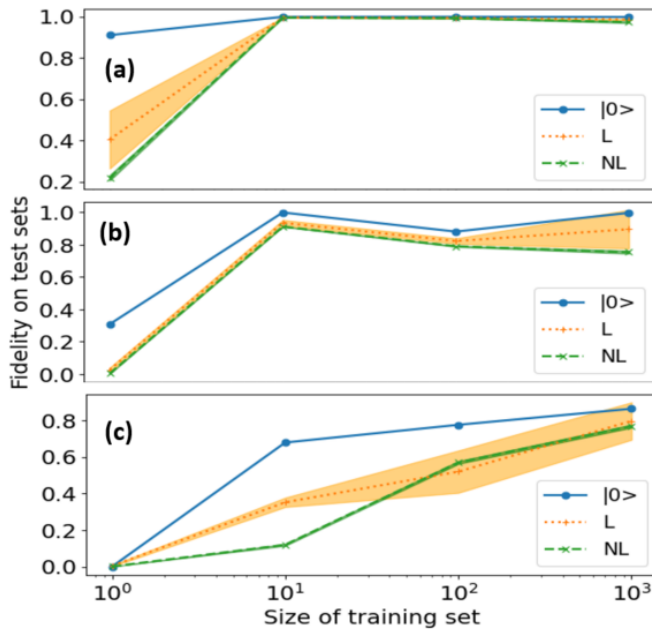


FIG. 6. Generalization error on different test sets, for circuit configurations initialised at increasing distances (a) 0.05, (b) 0.1 and (c) 0.15 ( $\times \pi \sqrt{2N_q D}$ ) from the known optimum. Training was done with  $n_{shots} = 2000$  circuit runs per rollout. Larger training sets demanded more control of the learning rate to improve, and the number of iterations ranged from a few hundred (for a training set with only one initial state) to a maximum of 5000 iterations (for 1000 initial states). The local test set was made of 100 states of the form  $\bigotimes_j^{10} |\xi\rangle_j$  where  $|\xi\rangle_j$ s are random qubit states, whereas the non-local test set was made of 100 random state vectors

in the training set grows, in accordance with calculations in Appendix B.

## V. CONCLUSION

We have introduced a method to compile variational quantum circuits using techniques from reinforcement learning. This approach constitutes an alternative gradient-free methods, and has the potential to outperform them at the onset of a barren plateau. This is be-

cause the optimization is not performed over  $\theta$ -space, but rather in the space of statistical distributions over  $\theta$ , for which it is possible to implement classical gradient ascent methods for the distribution parameters ( $\mu$  in our Gaussian case). A differentiable expression for the cost allows to estimate the gradient via non-local evaluations of the cost function.

Another salient feature of PG for variational compilation is that its performance is robust to noise. This crucial property allows us to achieve better performances in simulations with depolarizing noise strengths which are commensurate with state-of-the-art gate fidelities [49–52].

This method has the potential to be used as an efficient way to train shallow quantum circuits (for up to about a few tens of qubits) in the presence of noise, which could in turn be used as building blocks for larger circuits. An intriguing question is whether this method could be used as the lowest level of recursion in compilers reliant on the Solovay-Kitaev construction, where it could be used to replace the need for a library of gate sequences (along the lines of [35]). Improvements to the method introduced in this work could combine temporal difference learning with policy gradient, such as actor-critic methods, which could be used to train circuits layerwise (similarly to what is done in [39] and [26]).

While it is difficult to compare the runtimes of different approaches, we found that for a fixed performance threshold, PG-based approximate compilation is typically more efficient both in terms of absolute time and number of queries to a quantum computer. This is remarkably the case for larger circuits and in the presence of depolarizing noise.

Finally, we expect this RL-based approach to circuit training to be beneficial in quantum variational tasks other than unitary compilation. Quantum circuits with a number of parameters which grows mildly in the circuit depth, such as QAOA, are naturally better suited for this method more than quantum tasks in which the number of parameters is linear or polynomial in the depth.

## VI. CODE AVAILABILITY

Part of the code used to generate these results is available upon reasonable request.

- 
- [1] Nielsen M. A. & Chuang I. Quantum Computation and Quantum Information (2002)
  - [2] Harrow A. W., Recht B. & Chuang I. L. Efficient discrete approximations of quantum gates. *Journal of Mathematical Physics*, 43(9), 4445-4451 (2002)
  - [3] Dawson C. M. & Nielsen M. A. The Solovay-Kitaev algorithm. *arXiv preprint quant-ph/0505030* (2005)
  - [4] Lin H. W. Cayley graphs and complexity geometry. *Journal of High Energy Physics*, 2019(2), 1-15 (2019)
  - [5] Krioukov D., Papadopoulos F., Kitsak M., Vahdat A. & Boguná M. Hyperbolic geometry of complex networks. *Physical Review E*, 82(3), 036106 (2010)
  - [6] Nielsen M. A., Dowling M. R., Gu M. & Doherty A. C. Quantum computation as geometry. *Science*, 311(5764), 1133-1135 (2006)
  - [7] Preskill J. Quantum computing in the NISQ era and beyond. *Quantum*, 2, 79 (2018)
  - [8] Lloyd S. Quantum approximate optimization is computationally universal. *arXiv preprint arXiv:1812.11075*

- (2018)
- [9] Morales M. E., Biamonte J. D. & Zimborás Z. On the universality of the quantum approximate optimization algorithm. *Quantum Information Processing*, 19(9), 1-26 (2020)
  - [10] Kiani B., Maity R. & Lloyd S. Learning unitaries via gradient descent optimization. *Bulletin of the American Physical Society*, 65 (2020)
  - [11] Farhi E. & Harrow A. W. Quantum supremacy through the quantum approximate optimization algorithm. *arXiv preprint arXiv:1602.07674* (2016)
  - [12] Arute F., Arya K., Babbush R., Bacon D., Bardin J. C., Barends R., ... & Martinis J. M. Quantum supremacy using a programmable superconducting processor. *Nature*, 574(7779), 505-510 (2019)
  - [13] Zhu Q., Cao S., Chen F., Chen M. C., Chen X., Chung T. H., ... & Pan J. W. Quantum Computational Advantage via 60-Qubit 24-Cycle Random Circuit Sampling. *arXiv preprint arXiv:2109.03494* (2021)
  - [14] Bravyi S., Gosset D., & König R. Quantum advantage with shallow circuits. *Science*, 362(6412), 308-311 (2018)
  - [15] Bravyi S., Gosset D., Koenig R. & Tomamichel, M. Quantum advantage with noisy shallow circuits. *Nature Physics*, 16(10), 1040-1045 (2020)
  - [16] Bauer B., Bravyi S., Motta M. & Chan G. K. L. Quantum algorithms for quantum chemistry and quantum materials science. *Chemical Reviews*, 120(22), 12685-12717 (2020)
  - [17] O'Malley P. J., Babbush R., Kivlichan I. D., Romero J., McClean J. R., Barends R., ... & Martinis J. M. Scalable quantum simulation of molecular energies. *Physical Review X*, 6(3), 031007 (2016)
  - [18] Ralli A., Love P. J., Tranter A., & Coveney P. V. Implementation of measurement reduction for the variational quantum eigensolver. *Physical Review Research*, 3(3), 033195 (2021)
  - [19] Hastings M. B. Classical and quantum bounded depth approximation algorithms. *arXiv preprint arXiv:1905.07047* (2019)
  - [20] Bravyi S., Kliesch A., Koenig R., & Tang E. Obstacles to variational quantum optimization from symmetry protection. *Physical Review Letters*, 125(26), 260505 (2020)
  - [21] Bravyi S., Kliesch A., Koenig R. & Tang E. Hybrid quantum-classical algorithms for approximate graph coloring. *arXiv preprint arXiv:2011.13420* (2020)
  - [22] McClean J. R., Boixo S., Smelyanskiy V. N., Babbush R. & Neven, H. Barren plateaus in quantum neural network training landscapes. *Nature communications*, 9(1), 1-6 (2018)
  - [23] Cerezo M., Sone A., Volkoff T., Cincio L. & Coles P. J. Cost function-dependent barren plateaus in shallow quantum neural networks. *arXiv e-prints*, arXiv:2001 (2020)
  - [24] Grant E., Wossnig L., Ostaszewski M. & Benedetti, M. An initialization strategy for addressing barren plateaus in parametrized quantum circuits. *Quantum*, 3, 214 (2019)
  - [25] Volkoff T. & Coles P. J. . Large gradients via correlation in random parameterized quantum circuits. *Quantum Science and Technology*, 6(2), 025008 (2021)
  - [26] Skolik A., McClean J. R., Mohseni M., van der Smagt P. & Leib, M. Layerwise learning for quantum neural networks. *Quantum Machine Intelligence*, 3(1), (2021)
  - [27] Khatri S., LaRose R., Poremba A., Cincio L., Sornborger A. T., & Coles, P. J. Quantum-assisted quantum compiling. *Quantum*, 3, 140 (2019)
  - [28] Sharma K., Khatri S., Cerezo M. & Coles P. J. Noise resilience of variational quantum compiling. *New Journal of Physics*, 22(4), 043006 (2020)
  - [29] Wang S., Fontana E., Cerezo M., Sharma K., Sone A., Cincio L. & Coles P. J. Noise-induced barren plateaus in variational quantum algorithms. *Nature communications*, 12(1) (2021)
  - [30] Arrasmith A., Cerezo M., Czarnik P., Cincio L. & Coles P. J. Effect of barren plateaus on gradient-free optimization. *Quantum*, 5, 558 (2021)
  - [31] Schuld M., Bergholm V., Gogolin C., Izaac J. & Killoran, N. Evaluating analytic gradients on quantum hardware. *Physical Review A*, 99(3) (2019)
  - [32] Holmes Z., Arrasmith A., Yan B., Coles P. J., Albrecht A. & Sornborger A. T. Barren plateaus preclude learning scramblers. *Physical Review Letters*, 126(19), 190501 (2021)
  - [33] Sutton R. S. & Barto A. G. Reinforcement learning: An introduction. MIT press (2018)
  - [34] Nautrup H. P., Delfosse N., Dunjko V., Briegel H. J. & Friis N. Optimizing quantum error correction codes with reinforcement learning. *Quantum*, 3, 215 (2019)
  - [35] Moro, L., Paris, M. G., Restelli, M., & Prati, E. Quantum Compiling by Deep Reinforcement Learning. *arXiv preprint arXiv:2105.15048* (2021)
  - [36] Fösel T., Tighineanu P., Weiss T. & Marquardt F. Reinforcement learning with neural networks for quantum feedback. *Physical Review X*, 8(3), 031084 (2018)
  - [37] August M. & Hernández-Lobato, J. M. Taking gradients through experiments: LSTMs and memory proximal policy optimization for black-box quantum control. *International Conference on High Performance Computing*, Springer (2018)
  - [38] Porotti R., Essig A., Huard B. & Marquardt F. Deep Reinforcement Learning for Quantum State Preparation with Weak Nonlinear Measurements. *arXiv preprint arXiv:2107.08816* (2021)
  - [39] Garcia-Saez A. & Riu J. Quantum observables for continuous control of the quantum approximate optimization algorithm via reinforcement learning. *arXiv preprint arXiv:1911.09682* (2019)
  - [40] Yao J., Bukov M. & Lin, L.. Policy gradient based quantum approximate optimization algorithm. In *Mathematical and Scientific Machine Learning* (pp. 605-634). PMLR (2020)
  - [41] Yao J., Lin L., & Bukov M. Reinforcement Learning for Many-Body Ground State Preparation based on Counter-Diabatic Driving. *arXiv preprint arXiv:2010.03655* (2020)
  - [42] He Z., Li L., Zheng S., Li Y. & Situ H. Variational quantum compiling with double Q-learning. *New Journal of Physics*, 23(3), 033002 (2021)
  - [43] Blei D. M., Kucukelbir A. & McAuliffe J. D. Variational inference: A review for statisticians. *Journal of the American statistical Association*, 112(518), 859-877 (2017)
  - [44] Koller D. & Friedman N. Probabilistic graphical models: principles and techniques. MIT press (2009)
  - [45] Williams R. J. Simple statistical gradient-following algorithms for connectionist reinforcement learning. *Machine learning*, 8(3), 229-256 (1992)



- [46] Cirq, a python framework for creating, editing, and invoking noisy intermediate scale quantum NISQ circuits [github.com/quantumlib/Cirq](https://github.com/quantumlib/Cirq)
- [47] Shahriari B., Swersky K., Wang Z., Adams R. P. & De Freitas N. Taking the human out of the loop: A review of Bayesian optimization. *Proceedings of the IEEE*, 104(1), 148-175 (2015)
- [48] Colless J. I., Ramasesh V. V., Dahlen D., Blok M. S., Kimchi-Schwartz M. E., McClean, J. R., ... & Siddiqi I. Computation of molecular spectra on a quantum processor with an error-resilient algorithm. *Physical Review X*, 8(1), 011021 (2018)
- [49] Barends R., Kelly J., Megrant A., Veitia A., Sank D., Jeffrey E., ... & Martinis J. M. Superconducting quantum circuits at the surface code threshold for fault tolerance. *Nature*, 508(7497), 500-503 (2014)
- [50] Yang C. H., Chan K. W., Harper R., Huang W., Evans T., Hwang J. C. C., ... & Dzurak A. S. Silicon qubit fidelities approaching incoherent noise limits via pulse engineering. *Nature Electronics*, 2(4), 151-158 (2019)
- [51] Huang W., Yang C. H., Chan K. W., Tantt T., Hensen B., Leon R. C. C., ... & Dzurak A. S. Fidelity benchmarks for two-qubit gates in silicon. *Nature*, 569(7757), 532-536 (2019)
- [52] Schäfer V. M., Ballance C. J., Thirumalai K., Stephenson L. J., Ballance T. G., Steane A. M., & Lucas D. M. Fast quantum logic gates with trapped-ion qubits. *Nature*, 555(7694), 75-78 (2018)
- [53] Goodfellow I., Bengio Y. & Courville, A. *Deep Learning*. MIT press (2016)

## Appendices

### APPENDIX A: POLICY GRADIENT WITH GAUSSIAN POLICIES AND RMSPROP

The first step towards phrasing our approximate compilation problem as a reinforcement learning problem is to map the process of training a variational quantum circuit to a Markov Decision Process (MDP). Different mappings will lead to different learning scenarios in which distinct facets or challenges of the original quantum task will become apparent. An MDP consists of a tuple  $(\mathcal{S}, \mathcal{A}, R_{s,a}, P_{s',(s,a)},)$ , with  $\mathcal{S}$  the set of states,  $\mathcal{A}$  the set of actions,  $R$  is the reward obtained by taking action  $a$  in state  $s$ , and finally  $P$  is a stochastic matrix giving the probability of transitioning to state  $s'$  given that the current state is  $s$  and the current action is  $a$ . Generally,  $P$  is so large that it can only be sampled by an agent exploring an environment. An agent seeking to maximize the long-term reward of an MDP can do so by optimizing a policy  $\pi(a, s)$ , which associates a probability to each available action-state pair.

There exist several approaches to optimizing a policy. Temporal Difference methods aim at measuring the reward after each transition and update the value of each state under the current policy (the estimated long-term reward associated to that state). Optimality of the corresponding policies is ensured by the Bellmann Optimality Condition [33]. Another approach is given by the direct optimization of the policy, thus relying little, or not at all, on value iteration. One of the simplest policy gradient algorithms, conceptually as well as in terms of implementation, is the REINFORCE algorithm [45]. In REINFORCE, the policy is parameterized and belongs to a variational family of distributions, such that it is possible to differentiate it with respect to the variational parameters.

#### Reinforce with Endpoint Rewards

Throughout this work we have used a variation of the REINFORCE algorithm in which the reward will only be obtained at the end of a given sequence of actions (an episode). The motivation for this choice is ease of comparison with gradient-free optimisers, as explained in the main text. The rewards gathered at the end of each episode are used to estimate the gradient as follows: at each iteration the agent performs a Monte-Carlo tree search, i.e. it explores the space of actions for a fixed amount of time.

$$J = \mathbb{E}_{\pi_{\mu, \Sigma}}[R] = \sum_{\theta} \sum_k^m p_k \pi(\theta | \mu, \Sigma) r_{\theta}^{(k)}, \quad (6)$$

where we start at state  $s$  with probability  $p_k$  and the reward  $r_{\theta}^{(k)} = |\langle k | V(\theta)^{\dagger} U | k \rangle|^2$  is related to the end-state fidelity. Now the problem is to compute the gradient of this expectation value. Each particular trajectory in the Monte-Carlo tree search, a *rollout* in the RL jargon, contributes with a weight which is proportional to its associated final reward. This can be seen by applying the chain rule to the policy function:

$$\nabla_{\xi} J = \sum_{\theta} \sum_k^m p_k \pi(\theta | \mu, \Sigma) \nabla_{\xi} \log \pi(\theta | \mu, \Sigma) r_{\theta}^{(k)} \quad (7)$$

where  $\xi \in \{\mu, \Sigma\}$  and we have used the Gaussian policy:

$$\pi(x; \mu, \Sigma) = \frac{1}{\sqrt{2\pi|\Sigma|}} e^{-(x-\mu)\Sigma^{-1}(x-\mu)^T} \quad (8)$$

The ‘‘Log-likelihood trick’’ allows us to express a gradient of an expectation value as the expectation value of a different gradient, which can be estimated numerically. The logarithm of the Gaussian policy has the following gradients:

$$\nabla_{\mu} \log \pi(x; \mu, \Sigma) = \Sigma^{-1}(x - \mu) \quad (9)$$

$$\nabla_{\Sigma} \log \pi(x; \mu, \Sigma) = -\frac{1}{2} \Sigma^{-1} (\mathbf{1} - (x - \mu)^T (x - \mu) \Sigma^{-1}) \quad (10)$$

which allow for learning both the mean  $\mu$  and the covariance  $\Sigma$ . However, in this work we do not learn  $\Sigma$  but rather fix a simple exploration-exploitation schedule  $\Sigma(t) = (1 - t/T)\Sigma_i + t/T\Sigma_f$ , such that  $\Sigma_i \gg \Sigma_f \rightarrow 0$ .

### Reinforce with Intermediate Rewards

One possible improvement over REINFORCE with endpoint rewards is to perform intermediate measurements of the quantum state. The overhead incurred by this method is proportional to the number of layers, so in our case we argue that this is a reasonable cost. If we do perform projective measurements onto the wavefunction after each layer  $V^{(layers)}(\vec{\theta}_s)$  of the  $V(\vec{\theta}_T) = V^{(layerD)}(\vec{\theta}_3) \circ \dots \circ V^{(layer2)}(\vec{\theta}_2) \circ V^{(layer1)}(\vec{\theta}_1)$  circuit, such that  $\vec{\theta}_T = [\vec{\theta}_1, \vec{\theta}_2, \dots, \vec{\theta}_D]$ , then the generalised cost function is:

$$J_{LW} = \mathbb{E}_{\pi_{\mu, \Sigma}}[R] = \sum_k^m p_k \sum_s^D \sum_{\theta_s} \pi(\theta_s | \mu_s, \Sigma_s) G_s^{(k)}, \quad (11)$$

where LW stands for layerwise and the index  $s$  denotes the layer after which the fidelity is evaluated, ranging from 1 to a maximum depth  $D \propto \log N_q$  and the generalized return is  $G_s^{(k)} = \frac{1}{D-s+1} \sum_{s' > s}^D \gamma^{s'-s} |\langle k | V(\theta_s)^\dagger U | k \rangle|^2$ . The gradient is taken layerwise:

$$\nabla_{\mu_s} J_{LW} = \mathbb{E}_{\pi_{\mu_s, \Sigma_s}}[R] = \sum_k^m p_k \sum_s^D \sum_{\theta_s} \pi(\theta_s | \mu_s, \Sigma_s) \nabla_{\mu_s} \log \pi(\theta_s | \mu_s, \Sigma_s) G_s^{(k)}, \quad (12)$$

Setting  $\gamma = 1$  correspond to a far-sighted policy, which incentivates the  $V(\vec{\theta}_T)$  circuit to “unscramble” the computation as much as possible at each step while keeping a concerted global action. This strategy is similar in spirit to that followed in [39], in which the state of the RL agent corresponds to the wavefunction and has to be measured after each set of actions to sample the reward. Measuring the reward after each layer, for logarithmic depth circuits is a relatively low overhead and it has the potential to lead to higher performances, especially if supplemented with temporal-difference techniques.

### RMSprop and Baseline

Once the gradient has been estimated, the updates are performed following a *RMSprop* gradient update rule [53]. RMSprop is an adaptive learning rate method with empirically better convergence properties than simple gradient ascent methods. It works by (i) computing a discounted moving average of the gradient variances and (ii) dividing the update step by the discounted variance. The result is that the learning rate will increase in relatively flat landscape directions and it will decrease in steep landscapes. Let  $\sigma_g^2$  be the variance of the computed gradients over different rollouts.

$$\sigma_g^{(t)} = \gamma \sigma_g^{(t-1)} + (1 - \gamma) (\nabla_\xi J|_g)^2 \quad (13)$$

$$\xi \leftarrow \xi + \eta \frac{\nabla_\xi J|_g}{\sqrt{\sigma_g^{(t)} + \varepsilon}} \quad (14)$$

where  $\gamma$  is the discount factor. It has been empirically shown to allow for a more efficient exploration of complex cost landscapes. A list with the parameters used for this work is provided below:

Parameter	Value
$\Sigma_i$	$diag(5 \times 10^{-3})$
$\Sigma_f$	$diag(10^{-6})$
$N_{episodes}$	5-10
$p_s$	1/m
m	$n^2$
$\gamma$	0.9
$\eta$	$5 \times 10^{-3} - 1 \times 10^{-4}$
$\varepsilon$	$10^{-8}$
$maxiter_{\text{REINFORCE}}$	1000 – 10000
$maxiter_{\text{COBYLA}}$	10000
$maxiter_{\text{Powell}}$	30000

A further consideration is the choice of the baseline in the computation of the gradient, which allows to reduce the variance of the estimator. Provided the baseline is positively correlated with the end reward, i.e. if  $Cov[R, b] > 0$ , the advantage  $R - b$  will have less variance as the baseline will compensate the fluctuations of  $R$ . We have used a simple mean, i.e.  $b = \frac{1}{m} \sum_{\theta} r_{\theta}$ , which intuitively gives an advantage for the rollouts which perform better than average. Reducing the training error involves tuning all the hyperparameters of the policy gradient algorithm, for which there are several prescriptions to follow [47].

## APPENDIX B: EFFICIENT TRAINABILITY WITHOUT TOMOGRAPHICALLY COMPLETE MEASUREMENTS

It is in principle possible to efficiently calculate the fidelity at the end of each Monte-Carlo rollout by means of the so-called Hilbert-Schmidt test [27, 28], which makes use of an array of ancilla qubits and a series of potentially long range interactions.

In the absence of a secondary qubit register, one needs to resort to an estimation of the fidelity via Eq.(1). In the noiseless case, it is possible to recover the exact averaged value of the fidelity  $F(\theta) = \frac{1}{4^n} \sum_k^{\sim 4^n} |\langle k | V(\theta)^\dagger U | k \rangle|^2$  using a tomographically complete characterization.

An important consideration, therefore, is to ensure that our estimate of the fidelity  $\hat{F}(\theta)$ , which makes use of a massively downsampled subensemble of orthogonal states, is sufficient to train our variational circuit.

The set of initial states,  $\{|k\rangle\}^m$  with  $\langle k_i | k_j \rangle = \delta_{ij}$ , allows us to build an estimator  $\hat{F} = \frac{1}{m} \sum_k^m f_i$ , where  $0 \leq f_i \leq 1$  can be interpreted as independent samples of the true fidelity. In the limit where the fluctuations due to finite sampling vanish (infinitely many repetitions for each Monte-Carlo rollout), the Hoeffding inequality implies:

$$P(|\hat{F} - F| \geq \epsilon) \leq 2 \exp -2\epsilon^2 m \quad (15)$$

For large numbers of qubits, small differences of fidelity become increasingly significant and difficult to obtain through numerical optimization, which amounts to imposing a scaling on the estimator accuracy,  $\epsilon \sim n^{-t}$  for some positive real  $t$ . To satisfy the regime  $\epsilon^2 m \gg 1$  for any number of qubits gives a scaling of  $m \sim \Omega(n^{2t})$ .

## APPENDIX C: N-DIMENSIONAL RANDOM WALK

We will now present some basic facts about random walks in high-dimensional spaces, as this is the regime that describes a stalled optimization deep inside a barren plateau. Within an exponentially flat landscape and under a Gaussian policy, the estimator of the gradient can be written as:

$$\nabla_{\mu}^{\wedge} J = \frac{1}{N_{eps}} \sum_{\theta}^{N_{eps}} [\Sigma^{-1}(\theta - \mu)] \times \epsilon \quad (16)$$

where  $\epsilon$  corresponds to the reward (fidelity). The expected displacement at each iteration will be  $\delta\mu = \eta \nabla_{\mu}^{\wedge} J$ , whose covariance can be calculated to be  $CoVar[\delta\mu] = \eta^2 \epsilon^2 \Sigma^{-2} \hat{\Sigma} \approx \eta^2 \epsilon^2 \Sigma^{-1}$ . It is at first surprising that the variance of the expected displacement is inversely proportional to the initial covariance matrix. This is due to the fact that, in a Gaussian policy, the update rule is proportional to the reward but inversely proportional to the variance of exploration. Were this not the case, angles that are selected more frequently (as directions in  $\theta$ -space with larger variances will be sampled more frequently) might push the learning in a direction which is not that of the highest returns. This can be traced back to the relation between the logarithm of the parameterized Gaussian and the inverse probability of an action under a fixed policy[33].

For independent updates, i.e.  $\langle \delta\mu_{(i)} \delta\mu_{(j)} \rangle = \delta\mu_{(j)}^2 \delta_{ij}$ , at it is the case for REINFORCE in an exponentially flat region, one can express Mean Square Displacement (MSD) of the resulting random walk as:

$$\begin{aligned}
MSD^2 &= \langle (\sum_j^{N_{iters}} \delta\mu_{(j)})^2 \rangle = \langle \sum_j^{N_{iters}} \delta\mu_{(j)}^2 \rangle = \sum_j^{N_{iters}} \langle \delta\mu_{(j)}^2 \rangle \\
&= N_{iters} \frac{\eta^2 \epsilon^2}{N_{eps}^2} \langle [\sum_{ij} \text{Tr} \Sigma^{-2} (\theta_i - \mu)(\theta_j - \mu)^T] \rangle \\
&\approx N_{iters} \frac{\eta^2 \epsilon^2}{N_{eps}} \text{Tr} \Sigma^{-1} \\
&\leq N_{iters} \frac{\eta^2 \epsilon^2}{N_{eps}} \frac{2N_q D}{\sigma_{MIN}^2}
\end{aligned} \tag{17}$$

where the angle brackets denote an ensemble average. The number of free parameters is  $n_{params} = 2N_q D$  and  $\sigma_{MIN}^2$  is the minimum variance across all dimensions within the policy. The fact that the inverse of the covariance appears in the MSD calculation might seem counterintuitive, as one would expect a diffusive process to be proportional to the strength of the fluctuations rather than to their inverse. However, as explained above, the update rule given by the gradient estimator involves weighing by the inverse of the covariance to compensate for actions that are too likely to happen under the current policy.

This diffusive character of the optimization can be interpreted as a local search in a  $n_{params}$ -dimensional neighborhood performed by a random walker. The radius of the explored hyperball grows with the square root of the number of iterations. However, in high-dimensional spaces, the volume ratio between a hyperball of typical dimension  $\propto \sqrt{N_{iters}}$  and the corresponding hypercube vanishes as  $\pi^{n_{params}/2} / \Gamma(\frac{n_{params}}{2} + 1)$ , with  $\Gamma(x)$  the Euler's gamma, which is the reason why local search stalls deep inside in a barren plateau.

#### APPENDIX D: ERROR PROPAGATION FOR DEPOLARIZING CHANNEL

In our error model, the depolarizing channel  $\hat{C}_p \rho = (1-p)\rho + pI/2$  acts on each qubit after every single-qubit gate, giving rise to an effective noise rate  $p_{eff} = 1 - (1-p)^{N_q D}$ , with  $N_q$  the number of qubits and  $D \sim \log N_q$  the depth of the circuit. Then, the fidelity measured for a single episode in each PG iteration is expected to be damped according to:

$$F_{noisy} \propto (1 - p_{eff}) F_{noiseless} \tag{18}$$

This simple phenomenological model gives rise to a gradient update rule that is unbiased with respect to the noiseless one, with deviations that decrease proportionally to the square root of the number of shots (circuit repetitions).

The ratio  $\alpha = |\delta\mu_{noisy} \delta\mu_{noiseless}| / |\delta\mu_{noisy}| |\delta\mu_{noiseless}|$  can be used to compare the noisy update rule to the noiseless one. Considering  $\hat{p}(\theta) = n_{errors}^{(\theta)} / n_{shots}$ , where  $n_{errors}^{(\theta)}$  corresponds to the number of depolarizing errors in a particular instantiation of a circuit gate, and furthermore considering that for Gaussian policies one can express an update as  $\delta\mu_{noiseless} = \eta / N_{eps} \sum_i [\sum_\theta F_\theta \Sigma^{-1} (\mu - \theta)]_i$  where  $[\dots]_i$  is an unnormalized coordinate vector and  $F_\theta$  is the fidelity corresponding to a given circuit/episode:

$$\begin{aligned}
\mathbb{E}[\alpha] &= \mathbb{E} \frac{\eta^2 / N_{eps}^2 \sum_i [\sum_\theta (1 - \hat{p}(\theta))^{N_q D} F_\theta \Sigma^{-1} (\mu - \theta)]_i \cdot [\sum_\theta F_\theta \Sigma^{-1} (\mu - \theta)]_i}{|\delta\mu_{noisy}| |\delta\mu_{noiseless}|} \\
&= \frac{\eta^2 / N_{eps}^2 (1-p)^{N_q D} \sum_i [\sum_\theta F_\theta \Sigma^{-1} (\mu - \theta)]_i^2}{(1-p)^{N_q D} |\delta\mu_{noiseless}|^2} \\
&= 1
\end{aligned} \tag{19}$$

since we are taking that  $\mathbb{E}\hat{p}(\theta) = p$  for all possible angle configurations. This means that on average, the noisy update points in the correct direction, which is because the fidelity is assumed to be damped by the same ratio for all angles. Error propagation gives:

$$\Delta F_{noisy} = |\partial F_{noisy} / \partial p| \Delta p \propto N_q D p (1-p) \frac{\sigma_F}{\sqrt{N_{shots}}} \tag{20}$$

with  $\sigma_F$  arising from quantum noise. Increasing the number of repetitions will therefore narrow down the variance at each step in the gradient update.

This reasoning is not expected to hold for noise models where  $\mathbb{E}\hat{p}(\theta)$  is not independent of the angles (for instance for the low-temperature amplitude damping channel).